

# Multimedia Content Delivery in Millimeter Wave Home Networks

Bojiang Ma, *Student Member, IEEE*, Hamed Shah-Mansouri *Member, IEEE*,  
and Vincent W.S. Wong, *Fellow, IEEE*

**Abstract**—Millimeter wave (mm-wave) communication is a promising technology for short range communications and high speed services. It provides potential solutions for multimedia content delivery in home networks. However, approaches for resource allocation in traditional wireless networks may not be efficient for multimedia data transmissions in mm-wave networks. This is due to the very wide bandwidth and highly directional transmissions, which bring challenges as well as opportunities to the resource allocation of mm-wave transmissions. In this paper, we first characterize different usage scenarios of multimedia content delivery by introducing a set of utility functions. We then formulate a joint power and channel allocation problem based on a network utility maximization framework, which captures the spatial and frequency reuse of mm-wave communications. The formulated problem is a non-convex mixed integer programming (MIP) problem. We reformulate the problem into a convex MIP problem and propose a resource allocation algorithm based on outer approximation (OA) method. We further develop an efficient heuristic algorithm which has a lower complexity than the OA based algorithm. Simulation results present the tradeoffs between the OA based and heuristic algorithms for different scenarios and show that our proposed algorithms substantially outperform recently proposed schemes in the literature.

**Index Terms**—millimeter wave technology, smart home networks, spatial and spectrum reuse.

## I. INTRODUCTION

Home networks, which facilitate communications among devices inside a home, can improve the quality of life of the residents [1]. With the popularity of devices such as smart high-definition television (HDTV), tablets, and smartphones, multimedia content delivery has been a major source of data traffic in home networks. However, the number of devices and their traffic demand are increasing. It is important to improve the spectrum efficiency to better utilize the limited spectrum resources and meet the quality of service (QoS) requirement at the same time. The recently developed millimeter wave (mm-wave) band technology shows the potential to provide high data rate transmissions as well as high spectrum efficiency [2], [3]. The mm-wave technology can provide over 1 Gbps data rate for short range communication [4], which is promising

for multimedia content delivery [5], [6]. Since the mm-wave systems utilize directional transmissions [7], they result in small interfering ranges and can provide a good opportunity for spectrum reuse in smart home networks.

IEEE released the 802.15.3c [8] and 802.11ad [9] standards<sup>1</sup> for the wireless personal area network (WPAN) and wireless local area network (WLAN) based on mm-wave band technology. Both standards aim to enhance the throughput in the 60 GHz band. The applications include the support of wireless uncompressed video streaming, super broadband Internet access, and wireless office space in smart homes [10]. 802.15.3c and 802.11ad standards have similar medium access control (MAC) protocols. They have signalling period for control purpose, transmission coordination period for scheduling decision announcement, and data transfer interval. They use carrier sense multiple access with collision avoidance (CSMA/CA) for the contention-based access periods and time division multiple access (TDMA) for the reservation-based access periods. The IEEE 802.11ay [11], [12] study group is formed in 2015 to extend IEEE 802.11ad and further improve the throughput and different usage scenarios of mm-wave networks. However, the standardization process is still on going and stable documents are yet to be released.

Spectrum sharing and scheduling are important issues in resource allocation for mm-wave wireless networks. TDMA, frequency division multiple access (FDMA), and space division multiple access (SDMA) are three different multi-user access methods that schedule users with the shared resources. TDMA and FDMA eliminate interference among users by allocating non-overlapping resources. SDMA improves the system throughput by considering spatial reuse under interference control. TDMA has been used as the scheduling scheme for several industrial standards [8], [9], [13]. It can prevent co-channel interference and is simple to be implemented. However, TDMA does not fully exploit the spatial reuse and results in a low spectrum efficiency. Meanwhile, mm-wave technology adopts directional antennas which provide a significant opportunity to further utilize FDMA and SDMA. Considering the features of mm-wave, an integrated scheme, which employs SDMA together with FDMA and TDMA, can combine the benefits of each scheme and improve the spectrum efficiency.

<sup>1</sup>The IEEE 802.11ac which works on 5 GHz frequency band is also a good choice to satisfy the current demand of home networks. It can be regarded as an extension of 802.11a/g in terms of the MAC in 5 GHz band. In this paper, we focus on the mm-wave based home networks which can further satisfy the usage requirements in future home networks.

Manuscript received on Sept. 19, 2015; revised on Jan. 5, 2016; and accepted Mar. 13, 2016. This work was supported by the Natural Sciences and Engineering Research Council (NSERC) of Canada. The review of this paper was coordinated by Prof. Walid Saad.

Part of this paper was presented at the *IEEE Global Communications Conference (GLOBECOM14)*, Austin, TX, Dec. 2014.

B. Ma, H. Shah-Mansouri, and V. W. S. Wong are with the Department of Electrical and Computer Engineering, the University of British Columbia, Vancouver, BC, Canada, V6T 1Z4, e-mail: {bojiangm, hshahmansour, vincentw}@ece.ubc.ca.

There are several studies which investigate the wireless resource allocation problem in home networks. Wu *et al.* in [5] summarized the challenges of mm-wave multimedia communication in home networks and developed a QoS-aware multimedia scheduling scheme which achieves a balance between users' satisfaction and computational complexity. Yiakoumis *et al.* in [14] proposed a home network slicing control mechanism, which allows different service providers to deploy services using a shared infrastructure. They also presented a method to customize the slices for high-quality services. A resource reservation-based backoff mechanism is proposed in [15], which reuses time slots for transmission in backoff cycles to improve QoS for video delivery in home networks. In [16], Li *et al.* designed a distributed power control scheme with different radio access technologies, which aims to maximize the aggregate data rate of home networks. Sundaresan *et al.* in [17] developed a detection algorithm to locate the throughput bottlenecks in home networks. It uses timing and buffer information to accurately detect the bottlenecks in both cable and wireless links. Li *et al.* in [18] proposed a new rate adaptation scheme to reduce the latency for delay-sensitive applications in home networks.

Meanwhile, spatial reuse has been considered for mm-wave technology in several studies. Park *et al.* in [19] investigated the potentials for spatial reuse and interference management in mm-wave wireless networks and developed a simulation model to evaluate the spatial reuse performance. In [20], Chen *et al.* proposed a spatial reuse strategy for mm-wave WPANs with different directional antennas based on beamforming information. A scalable heuristic STDMA scheduling (SHSS) algorithm, which allows concurrent transmissions in the same time slot, is proposed in [21] to enhance the throughput of mm-wave based networks. In [22], Singh *et al.* investigated interference management for mm-wave mesh networks, and proposed an analytical framework to estimate the impact of antenna pattern and density of concurrent links on the MAC protocol. Qiao *et al.* in [23] formulated an optimization problem to maximize the aggregate throughput of indoor mm-wave networks by considering concurrent beamforming. They proposed an iterative beam searching algorithm, which increases the throughput and improves the energy efficiency of the system. Athanasiou *et al.* in [24] considered multi-user SDMA in client association problem and proposed an association algorithm based on subgradient methods.

Special characteristics of mm-wave communications (e.g., directional transmission via beamforming, low multiuser interference) have been utilized to improve various performance metrics. From the perspective of mm-wave local area networks, in [25], Shokri-Ghadikolaei *et al.* investigated the important challenges of MAC design in short range mm-wave networks. They showed that collision-aware MAC can improve the efficiency of mm-wave networks. In [26], Son *et al.* developed a directional MAC protocol to allow concurrent transmissions to exploit spatial reuse in mm-wave WPANs. Kim *et al.* in [27] considered the video transmission in a sport stadium using mm-wave technology and formulated a relay selection and coding rate adaptation problem to maximize the video quality. From the perspective of mm-wave

cellular networks, Zheng *et al.* in [28] studied the challenges and protocols in 5G mm-wave based cellular system. Their simulation results show the potential of achieving a very high capacity in the future mm-wave cellular systems. In [29], Di Renzo introduced a novel analysis framework using stochastic geometry for mm-wave cellular networks. The analysis and simulation showed that the noise-limited approximation is accurate for typical cellular network densities.

D2D communication based on mm-wave technology is an emerging topic and has great potentials in future mm-wave home networks. Niu *et al.* in [30] proposed a scheduling scheme for D2D transmissions to exploit spatial reuse in mm-wave heterogeneous cellular systems. In [31], Qiao *et al.* proposed a TDMA-based MAC structure and a resource sharing scheme for D2D communications in mm-wave based networks. Rehman *et al.* in [32] proposed a scheduling algorithm for mm-wave D2D networks using vertex coloring approach. Their method improved the aggregate throughput by scheduling the conflicting flows with different priority. Besides, the measurement results for mm-wave home networks are provided in [33]–[36].

Millimeter wave based technology is being regarded as a promising candidate for multimedia content delivery in home networks in the foreseeable future. However, the studies for multimedia transmission using mm-wave is limited. The existing resource allocation schemes in mm-wave networks do not capture the characteristics of various applications in mm-wave multimedia home networks. Although optimization framework has frequently been used to tackle the resource allocation problem for indoor wireless networks, there are several differences for the scheduling and power allocation problem using mm-wave. First, the propagation features of mm-wave transmission, such as high attenuation and sensitivity to blockage, makes it possible to utilize spatial reuse to further improve the spectrum efficiency. Second, the multiuser interference in directional communication in mm-wave transmission is substantially less than that in omnidirectional systems. Third, the characteristics of mm-wave create the specific constraints for the resource allocation, such as possible channel bonding. Moreover, the existing works do not fully exploit the diversity of frequency division, which can further improve the energy efficiency and channel utilization.

It is essential to design a novel scheduling mechanism to better utilize the special features of mm-wave communications (such as wide bandwidth, directional communication, small interfering range), and satisfy the new requirements for various types of multimedia content delivery (such as high data rate for uncompressed HD video transmission and flexible data rate for file downloading). It is also important to consider energy efficiency for growing number of battery-powered portable devices in home networks.

In this paper, we study the scheduling and power allocation problem in the emerging smart home networks based on mm-wave technology. We adopt directional antennas for practical mm-wave communications. We consider potential concurrent transmissions in the network, which deliver various types of multimedia content (e.g., uncompressed video). The main contributions of this paper are as follows:

- We introduce utility functions to characterize different usage scenarios and types of multimedia services in the smart home networks.
- We propose a novel integrated TDMA/FDMA/SDMA scheduling scheme that allows concurrent transmissions using directional antenna for mm-wave home network to fully exploit the potential of spatial reuse and further increase the spectrum efficiency.
- We formulate a channel and power allocation problem, which considers QoS and energy efficiency requirements of users, and maximizes the aggregate network utility. The formulated problem is a non-convex mixed integer programming (MIP) problem. We reformulate the non-convex problem into a convex MIP problem and design an algorithm based on the outer approximation (OA) method to obtain the optimal solution of the reformulated problem. We further propose a heuristic algorithm, which has a lower computational complexity than the OA based algorithm.
- Through extensive numerical studies, we evaluate the performance of our proposed algorithms in terms of aggregate utility and throughput for different home networks. We further compare both proposed algorithms with recently proposed scheduling algorithms [21] and [32]. Results show a substantial improvement in terms of aggregate throughput and utility compared with the proposed algorithms in [21] and [32].

The key differences between our work and [21] are as follows. In [21], the authors aimed to improve the system throughput. In this paper, we formulate a utility maximization problem to better characterize different application scenarios of multimedia content delivery in mm-wave networks. Furthermore, we consider the minimum data rate requirement and energy efficiency as the practical constraints in our formulation. The authors in [21] proposed a heuristic STDMA scheduling scheme, while we introduce an OA method to obtain the solution of the resource allocation problem. We further propose a greedy algorithm which has a lower complexity than the OA method. Results show that both of our algorithms outperform the one proposed in [21]. More importantly, we introduce channelization and possible channel bonding of 60 GHz bands to bring another dimension to further improve the spectrum efficiency of the mm-wave systems.

We extend the work in [37] from several aspects. In [37], we studied the resource allocation problem for multimedia content delivery using omni-directional mm-wave communication without spatial reuse. In this paper, we improve the spatial reuse by allowing concurrent transmissions in the same channel. We further consider more practical directional antennas for mm-wave communication instead of omni-directional antennas. We utilize the small interfering range feature of directional mm-wave communications and design an integrated scheduling scheme, which significantly improves the spectrum efficiency. We design a new algorithm based on the OA method, which has a lower computational complexity than the generalized Benders decomposition method used in [37]. We also propose a heuristic algorithm which is computationally

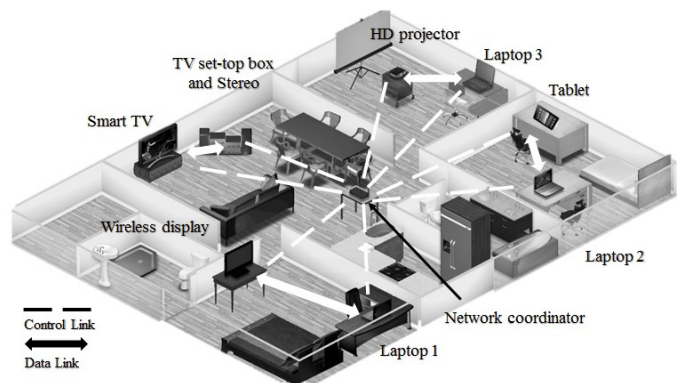


Fig. 1. An example of a smart home wireless network. Solid arrows represent the multimedia content delivery links. Dashed lines illustrate the control message exchange links. The access point also acts as a coordinator to schedule the transmissions among the device pairs.

less complex than the OA method.

The rest of this paper is organized as follows: In Section II, we present the system model. We formulate the resource allocation problem in Section III, and propose a scheduling algorithm in Section IV. We develop a low complexity heuristic algorithm in Section V. Simulation results are presented in Section VI. Conclusions are given in Section VII. The key notations and variables used in this paper are listed in Table I.

## II. SYSTEM MODEL

We consider a smart home network as shown in Fig. 1. The network devices are equipped with mm-wave technology. The list of devices includes smart HDTV, TV set-top box, laptops, HD projector, and wireless display. The devices are coordinated by the access point via the control links. The multimedia content is delivered via the data links. Each data link consists a transmitting device and a receiving device. We denote the set of data links by  $\mathcal{Q}$ , where each data link serves a different pair of users. We assume the multimedia contents, such as videos for wireless display and files to be shared, are available at the transmitting devices. Short control messages need to be exchanged between the access point and devices for resource allocation purpose. Note that the network setting is similar to the IEEE 802.15.3c and 802.11ad standards, which only allow one radio frequency (RF) chain between a pair of transmitter and receiver. If multiple RF chains are required for multimedia content sharing, the spatial gain can be limited by the number of RF chains that one device can create.

### A. Channel Model

We consider the mm-wave transmissions operate in the frequency band from 57 GHz to 64 GHz. This band is used in 802.15.3c [8], 802.11ad [9], and 802.11ay [11]. There are three channels in this frequency range according to the mm-wave band channelization. Each channel has a bandwidth of 2160 MHz. The channel model at the 60 GHz band is quite different from that for 2.4 or 5 GHz bands. One important difference is that the 60 GHz communication requires directional antenna. We adopt the wireless channel model in the 60 GHz

TABLE I  
LIST OF KEY NOTATIONS AND VARIABLES USED IN THIS PAPER

Symbols	Meaning
$B$	Bandwidth of each channel
$\mathcal{C}$	Set of available channels
$G_0$	Antenna gain of a pair of communicating devices
$G_{i,j}$	Antenna gain between transmitter $i$ and receiver $j$
$h_{i,j}^{t,c}$	Channel gain between transmitter $i$ and receiver $j$ in time slot $t$ on channel $c$
$I_i^{\max}$	Estimated maximum interference received by receiver $i$
$I_i^{t,c}$	Interference received by receiver $i$ in time slot $t$ on channel $c$
$L_{\text{slot}}$	Length of each time slot
$L_{\text{sp}}$	Length of scheduling period
$L_a$	Length of alignment period
$L_b$	Length of beacon period
$L_c$	Length of control period
$N_0$	Background noise power
$p_i^{t,c}$	Transmission power at transmitter $i$ in time slot $t$ on channel $c$
$p^{\max}$	Maximum transmission power
$\mathbf{p}$	Power allocation vector
$\mathcal{Q}$	Set of data links
$\mathcal{V}$	Set of data links with battery-powered transmitting devices
$\mathcal{Z}$	Set of data links with minimum data rate requirement
$r_i$	Effective throughput of link $i$
$\bar{r}_i$	Effective throughput of link $i$ when interference is limited to $I_i^{\max}$
$r_i^{\min}$	Minimum data rate requirement for link $i$
S1, S2, S3	Usage scenarios
$\mathcal{T}$	Set of time slots
$U_i$	Utility of user $i$
$\bar{U}_i$	Utility of user $i$ when interference is limited to $I_i^{\max}$
$x_i^{t,c}$	Time slot and channel allocation variable for link $i$ in time slot $t$ on channel $c$
$\mathbf{x}$	Time slot and channel allocation vector
$\eta$	Efficiency of transceiver
$\xi$	Threshold of energy efficiency
$\Theta_{3\text{dB}}$	Beam-level beam width
$\Psi^{\text{st}}$	Sector-level beam width for transmitter
$\Psi^{\text{sr}}$	Sector-level beam width for receiver

indoor situation [35], which is proposed specifically for mm-wave communication. Each transmitting antenna distributes the power in the main lobe and several side lobes. In this paper, we consider the large scale channel characterizations. Specifically, we consider the impact of blockage and reflections for both line-of-sight (LOS) and non-line-of-sight (NLOS) cases. If the LOS is blocked, we consider possible NLOS communications. This is because the first order reflection in mm-wave networks can be significant [38] and makes NLOS communication possible. The shadowing and multipath effects caused by blockage and reflections of mm-wave signals are included in the channel model [35, pp. 7] [36, pp. 141]. In the mm-wave channel model, the channel gain between the transmitter of link  $i$  and receiver of link  $j$  ( $i, j \in \mathcal{Q}$ ) is represented as  $h_{i,j} = \frac{1}{PL(d_{i,j})}$ , where  $d_{i,j}$  is the distance between the corresponding transmitter and receiver. The path

loss is given by [35]

$$PL(d)[\text{dB}] = \begin{cases} A_{\text{LOS}} + 10n_{\text{LOS}} \log_{10} \left( \frac{d}{d_{\text{bp}}} \right) + X_{\sigma_{\text{LOS}}} \\ + 20 \log_{10} \left( \frac{4\pi f_c d_{\text{bp}}}{s} \right), & \text{if LOS exists,} \\ A_{\text{NLOS}} + 10n_{\text{NLOS}} \log_{10} \left( \frac{d}{d_{\text{bp}}} \right) + X_{\sigma_{\text{NLOS}}} \\ + 20 \log_{10} \left( \frac{4\pi f_c d_{\text{bp}}}{s} \right), & \text{if LOS is blocked,} \end{cases} \quad (1)$$

where  $A_{\text{LOS}}$  and  $A_{\text{NLOS}}$  are the attenuation in LOS and NLOS signals,  $n_{\text{LOS}}$  and  $n_{\text{NLOS}}$  are the path loss exponents, and  $X_{\sigma_{\text{LOS}}}$  and  $X_{\sigma_{\text{NLOS}}}$  are zero-mean Gaussian random variables with standard deviation  $\sigma_{\text{LOS}}$  and  $\sigma_{\text{NLOS}}$  that model the shadowing effects of LOS and NLOS environments, respectively. In addition,  $f_c$  is the carrier frequency,  $d_{\text{bp}}$  is the reference distance, and  $s$  is the speed of light. Channel estimation helps to determine the aforementioned parameters. It is performed periodically by the transmitter and receiver via transmitting and analyzing orthogonal pilot sequences [39].

In mm-wave technology, directional antenna is used to improve the antenna gain. A directional transmitting antenna model is proposed in [40]. In this model, the transmitting antenna achieves a high gain in the main lobe and an averaged low gain in the side lobes. The antenna gain in different directions is given as follows [40]:

$$G^{\text{tx}}(\Theta^{\text{tx}}) = \begin{cases} G_0^{\text{tx}} 10^{-1.204(\Theta^{\text{tx}}/\Theta_{3\text{dB}})^2}, & \text{if } 0^\circ \leq \Theta^{\text{tx}} < \Theta_{\text{ml}}/2, \\ G_{\text{sl}}^{\text{tx}}, & \text{if } \Theta_{\text{ml}}/2 \leq \Theta^{\text{tx}} \leq 180^\circ, \end{cases} \quad (2)$$

where  $G_0^{\text{tx}}$  and  $G_{\text{sl}}^{\text{tx}}$  represent the maximum transmitting antenna gain and the average side lobe gain, respectively. The transmitting angle is denoted as  $\Theta^{\text{tx}}$ .  $\Theta_{3\text{dB}}$  is the angle of the half-power beam width, and  $\Theta_{\text{ml}}$  is the angle of the main lobe. In addition,  $G_0^{\text{tx}} = 10^{0.9602 - 2 \ln \sin(\Theta_{3\text{dB}}/2)}$ ,  $G_{\text{sl}}^{\text{tx}} = 10^{-0.04111 \ln \Theta_{3\text{dB}} - 1.0597}$ , and  $\Theta_{\text{ml}} = 2.6\Theta_{3\text{dB}}$ .

We consider the network devices are equipped with directional receiving antennas where the antenna models are the same as transmitting ones. The receiving antenna gain is denoted by  $G^{\text{rx}}(\Theta^{\text{rx}})$ . The receiving angle is denoted as  $\Theta^{\text{rx}}$ , which is the angle between the line from the signal source to the receiving antenna and the pointing direction of the antenna. The antenna gain for directional receiving antenna is given as follows:

$$G^{\text{rx}}(\Theta^{\text{rx}}) = \begin{cases} G_0^{\text{rx}} 10^{-1.204(\Theta^{\text{rx}}/\Theta_{3\text{dB}})^2}, & \text{if } 0^\circ \leq \Theta^{\text{rx}} < \Theta_{\text{r}}/2, \\ G_{\text{sl}}^{\text{rx}}, & \text{if } \Theta_{\text{r}}/2 \leq \Theta^{\text{rx}} \leq 180^\circ, \end{cases} \quad (3)$$

where  $G_0^{\text{rx}}$  and  $G_{\text{sl}}^{\text{rx}}$  represent the maximum receiving gain and the average side lobe gain, respectively, and  $\Theta_{\text{r}}$  is the angle of receiving range.

In Fig. 2, we show the transmission pattern using directional transmitting and receiving antennas. The directional beams of transmitters and receivers are shown by the oval-like shapes. Different grids represent the communication in different frequency bands. The antenna gain of each pair of communicating devices is denoted by  $G_0 = G^{\text{tx}}(0)G^{\text{rx}}(0)$ . We

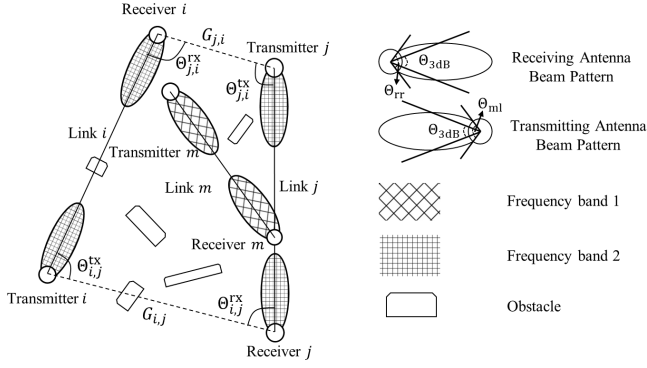


Fig. 2. An example of transmission pattern using directional transmitting and receiving antennas. The antenna patterns illustrate gains in different directions. The obstacles have different sizes and are located randomly. Frequency band 1 is allocated to link  $m$  to avoid possible interference with links  $i$  and  $j$ . Frequency band 2 is allocated to links  $i$  and  $j$  to improve spatial reuse.

denote the angle between lines from transmitter  $j$  to receivers  $i$  and  $j$  by  $\Theta_{j,i}^{rx}$ . Similarly, we denote the angle between lines from receiver  $i$  to transmitters  $j$  and  $i$  by  $\Theta_{j,i}^{tx}$ . The antenna gain between transmitter  $j$  and receiver  $i$  is denoted as  $G_{j,i} = G_{j,i}^{rx}(\Theta_{j,i}^{rx})G_{j,i}^{tx}(\Theta_{j,i}^{tx})$ .

### B. Integrated TDMA/FDMA/SDMA Scheduling for Smart Home Networks

In home networks, the access point also acts as the coordinator (similar to the piconet coordinator in WPAN and personal basic service set central point in WLAN). We propose an integrated scheduling scheme based on a scheduling period structure. Each scheduling period begins with a beacon period for network synchronization. It is followed by the control message exchanging period. During this period, transmitters can send the transmission request messages and the coordinator broadcasts the scheduling decision. The remaining time of the scheduling period is the data transfer interval. The multimedia content delivery usually has different QoS requirements. Therefore, QoS-constrained multimedia content is usually scheduled in the contention-free periods according to the standards. We assume all multimedia content is transferred using the reservation-based time slots in the data transfer interval. Each time slot starts with an alignment period, followed by the data transmission period. In both IEEE 802.15.3c and 802.11ad standards, TDMA is used during the reservation-based period, which only allows one transmission pair in a time slot. To further explore the spectral reuse for mm-wave technology, we allow co-channel concurrent transmissions in the same time slot using SDMA. To meet the QoS requirements of different services, such as wireless display or video gaming, the reservation-based period is centrally scheduled by the coordinator for each transmission pair.

In Fig. 3, we illustrate the structure of a scheduling period with the proposed integrated TDMA/FDMA/SDMA scheme. The scheduling period consists of the beacon, control, and data transfer interval. We use  $L_b$ ,  $L_c$ ,  $L_{slot}$ , and  $L_{sp}$  to denote the length of the beacon period, control period, time slot, and the scheduling period, respectively. In each time slot, we use  $L_a$  to

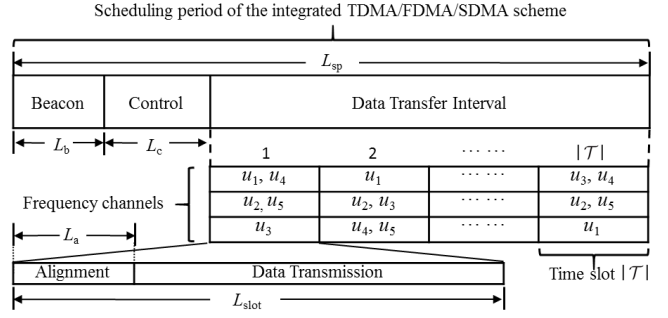


Fig. 3. Structure of the proposed integrated TDMA/FDMA/SDMA scheduling scheme for mm-wave home networks.

represent the duration of the alignment period. According to the standard [9, pp. 300], during the alignment period in data transfer interval, the beamforming refinement protocol (BRP) is executed for the alignment. Exhaustive search is used to find the refined beams. We define the sector-level beam width for the transmitter and receiver as  $\Psi^{st}$  and  $\Psi^{sr}$ , respectively. We also denote the time required to transmit pilot sequences as  $T_p$ . The overhead of the alignment can be modeled as  $L_a = \lceil \frac{\Psi^{st}}{\Theta_{3dB}} \rceil \lceil \frac{\Psi^{sr}}{\Theta_{3dB}} \rceil T_p$  [41], where  $\lceil \cdot \rceil$  is the ceiling function. Note that the beam-level beam width is  $\Theta_{3dB}$ .

In the data transfer interval, each device is allocated different channel and time slot. Different from WPAN/WLAN specifications 802.15.3c and 802.11ad, we allow different devices to occupy the same frequency band within the same time slot (e.g., users  $u_1$  and  $u_4$  in the first time slot and first frequency band) based on SDMA. FDMA is also integrated in scheduling mechanism by dividing the whole frequency band into three separate channels according to [8]. By integrating FDMA, more flexibility is provided for the scheduling mechanism to improve the channel utilization.

The coordinator is responsible for allocating the resource blocks to all links to optimize the network performance. We denote  $\mathcal{T}$  as the set of time slots, and  $\mathcal{C}$  as the set of available mm-wave frequency bands. We further denote  $p_i^{t,c}$  and  $h_{i,i}^{t,c}$  as the transmission power at the transmitting device of link  $i$  and the corresponding channel gain of the link on channel  $c \in \mathcal{C}$  in time slot  $t \in \mathcal{T}$ , respectively. We use  $\mathbf{p}_i = (p_i^{1,1}, \dots, p_i^{1,|\mathcal{C}|}, \dots, p_i^{|\mathcal{T}|,1}, \dots, p_i^{|\mathcal{T}|,|\mathcal{C}|})$  to denote the power allocation decision vector for the transmitting device of link  $i$ , and  $\mathbf{p} = (\mathbf{p}_1, \dots, \mathbf{p}_i, \dots, \mathbf{p}_{|\mathcal{Q}|})$  to denote the power allocation vector for all links. The effective throughput  $r_i$  for link  $i$  can be modeled as

$$r_i(\mathbf{p}) = \eta B \frac{L_{slot} - L_a}{L_{sp}} \sum_{t \in \mathcal{T}} \sum_{c \in \mathcal{C}} \log_2 \left( 1 + \frac{p_i^{t,c} G_0 h_{i,i}^{t,c}}{N_0 + I_i^{t,c}} \right), \quad (4)$$

where  $B$  is the bandwidth of each channel,  $\eta \in [0, 1]$  is the efficiency of the transceiver, and  $N_0$  is the noise power. In addition,  $I_i^{t,c} = \sum_{j \in \mathcal{Q} \setminus \{i\}} p_j^{t,c} G_{j,i} h_{j,i}^{t,c}$  is the received interference power of link  $i$  on channel  $c$  in time slot  $t$ .

### C. Utility Functions

Utility is considered as an important metric to efficiently allocate resource blocks to heterogeneous multimedia traffic.

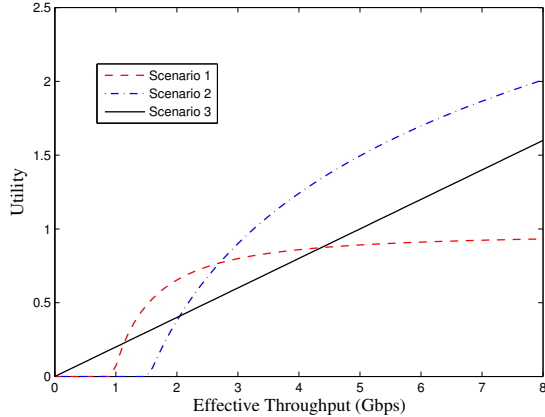


Fig. 4. An example of utility versus effective throughput for different scenarios.

The utility reflects the relative satisfaction level of a user regarding the allocated resources. We define utility functions to characterize the users' experience for different types of multimedia content delivery. We consider the following usage scenarios for mm-wave applications: S1) Uncompressed video streaming; HDTV signal transmission with adaptive modulation coding; S2) Workstation desktop and conference ad-hoc: transmissions between computer devices or in an ad-hoc manner; S3) Kiosk file downloading; video and music sharing on portable devices.

We define  $\mathcal{S}_1$ ,  $\mathcal{S}_2$ , and  $\mathcal{S}_3$  as the sets of users that use services under usage scenarios S1, S2 and S3, respectively. Some services in scenarios S1 and S2, such as video streaming or conference ad-hoc, have a minimum data rate requirement. Since each transmission link serves a corresponding user, we use set  $\mathcal{Q}$  to represent the set of the users as well as the links. In the remaining parts of the paper, we use the terms *link* and *user* interchangeably. We use the following quasi-concave function to characterize the satisfaction level of user  $i \in \mathcal{S}_1 \cup \mathcal{S}_2$  with respect to effective throughput:

$$U_i(r_i(\mathbf{p})) = \begin{cases} 0, & r_i(\mathbf{p}) < r_i^{\min}, \\ K_i^1 \ln(1 + K_i^2 \ln(1 + (r_i(\mathbf{p}) - r_i^{\min}))), & r_i(\mathbf{p}) \geq r_i^{\min}, \end{cases} \quad (5)$$

where coefficients  $K_i^1$  and  $K_i^2$  are application dependent parameters, and  $r_i^{\min}$  is the minimum data rate requirement for user  $i$  under specific usage scenario. The satisfaction of user  $i$  increases quickly at the beginning when  $r_i^{\min}$  is achieved and then the marginal increment becomes smaller as the data rate increases. This type of function is widely used for applications with minimum data rate requirement. The services in scenario S3, such as file downloading, do not have a minimum data rate requirement (i.e.,  $r_i^{\min} = 0, i \in \mathcal{S}_3$ ). Moreover, the utility increases linearly with respect to the effective throughput. For these services, we use the following linear utility function [42] for user  $i \in \mathcal{S}_3$  as follows:

$$U_i(r_i(\mathbf{p})) = K_i^3 r_i(\mathbf{p}), \quad (6)$$

where  $K_i^3$  is an application dependent parameter. Examples of utility functions for different scenarios are shown in Fig. 4.

### III. PROBLEM FORMULATION

The use of directional antenna can allow more concurrent transmissions. However, only a proper scheduling scheme can fully exploit the potentials of the spatial reuse. Therefore, we propose an integrated TDMA/FDMA/SDMA scheme, which considers spatial reuse of directional antenna and co-channel interference management in order to improve the spectrum efficiency of the home networks.

Apart from the benefits, the high power consumption of mm-wave communication brings a challenge to the battery-powered devices such as smartphones and tablets. Therefore, energy efficiency becomes a critical challenge for mm-wave based systems. We define the energy efficiency of user  $i$  as the ratio between the amount of data transmitted and the energy consumed, which is

$$\frac{L_{\text{sp}} r_i(\mathbf{p})}{(L_{\text{slot}} - L_a) \sum_{t \in \mathcal{T}} \sum_{c \in \mathcal{C}} p_i^{t,c}}, \quad (7)$$

where  $(L_{\text{slot}} - L_a) \sum_{t \in \mathcal{T}} \sum_{c \in \mathcal{C}} p_i^{t,c}$  represents the energy consumed by user  $i$  to transmit  $L_{\text{sp}} r_i(\mathbf{p})$  amount of data. We use  $\mathcal{V} \subset \mathcal{Q}$  to denote the set of links with battery-powered transmitting devices. We consider a threshold of the energy efficiency for these links in set  $\mathcal{V}$ .

To formulate the problem, we define binary variables  $x_i^{t,c} \in \{0, 1\}, t \in \mathcal{T}, c \in \mathcal{C}$ , where  $x_i^{t,c} = 1$  if time slot  $t$  in channel  $c$  is allocated to link  $i$ . Otherwise,  $x_i^{t,c} = 0$ . We also define time slot and channel allocation vector  $\mathbf{x}_i = (x_i^{1,1}, \dots, x_i^{1,|\mathcal{C}|}, \dots, x_i^{|\mathcal{T}|,1}, \dots, x_i^{|\mathcal{T}|,|\mathcal{C}|})$  for user  $i$ , and vector  $\mathbf{x} = (\mathbf{x}_1, \dots, \mathbf{x}_i, \dots, \mathbf{x}_{|\mathcal{Q}|})$  for all users. We consider the aggregate network utility as the performance criterion. The optimal resource allocation decision depends on the allocated resource blocks and the transmission power of the transmitting devices. We denote the maximum transmission power as  $p^{\max}$ . The threshold of energy efficiency is denoted by  $\xi$ . To find the optimal resource allocation decision, the utility maximization problem is formulated as follows:

$$\text{maximize}_{\mathbf{x}, \mathbf{p}} \sum_{i \in \mathcal{Q}} U_i(r_i(\mathbf{p})) \quad (8a)$$

$$\text{subject to } r_i(\mathbf{p}) \geq r_i^{\min}, \quad i \in \mathcal{Q}, \quad (8b)$$

$$r_i(\mathbf{p}) \geq \xi \frac{L_{\text{slot}} - L_a}{L_{\text{sp}}} \sum_{t \in \mathcal{T}} \sum_{c \in \mathcal{C}} p_i^{t,c}, \quad i \in \mathcal{V}, \quad (8c)$$

$$0 \leq p_i^{t,c} \leq x_i^{t,c} p^{\max}, \quad i \in \mathcal{Q}, t \in \mathcal{T}, c \in \mathcal{C}, \quad (8d)$$

$$\sum_{c \in \mathcal{C}} x_i^{t,c} \leq 3, \quad i \in \mathcal{Q}, t \in \mathcal{T}, \quad (8e)$$

$$x_i^{t,c} \in \{0, 1\}, \quad i \in \mathcal{Q}, t \in \mathcal{T}, c \in \mathcal{C}, \quad (8f)$$

where constraint (8b) ensures that the minimum throughput requirement is satisfied for each user. Constraint (8c) implies that the ratio between the effective throughput and power consumption is greater than the minimum threshold  $\xi$ . Constraint (8d) guarantees that the transmission power of link  $i$  is not greater than  $p^{\max}$ . According to the latest standardization progress of mm-wave networks (i.e., IEEE 802.11ay [11]), channel bonding is considered to allow each transmission pair to use up to three mm-wave channels in a time slot. Therefore,

we consider constraint (8e) to indicate that each link can utilize no more than three bonded channels during a time slot.

Note that the objective function in (8a) is non-convex due to the interference term  $I_i^{t,c}$  in (4). Moreover, the time slot and channel allocation variables  $\mathbf{x}$  are binary. Thus, problem (8) is a non-convex MIP problem, which is in general hard to solve. However, we can reformulate the problem and obtain a sub-optimal solution. To reformulate problem (8), we first evaluate the potential interference received by each link. Due to the directional communication of mm-wave networks, multiuser interference is greatly reduced compared with omni-directional systems. The mm-wave systems show a transitional behavior from interference-limited to noise-limited regime, depending on several factors such as density of transmitters and operating beam width [43]. The interference observed by different links may be completely different. In this paper, we estimate the interference for each link by assuming all links transmit in the same channel with maximum transmission power  $p^{\max}$ . The estimated interference of link  $i$  is denoted as  $I_i^{\max}$ . A similar idea is used in [41], which provides a conservative estimation of the interference. We define

$$\bar{r}_i(\mathbf{p}_i) \triangleq \eta B \frac{L_{\text{slot}} - L_a}{L_{\text{sp}}} \sum_{t \in \mathcal{T}} \sum_{c \in \mathcal{C}} \log_2 \left( 1 + \frac{p_i^{t,c} G_0 h_{i,i}^{t,c}}{N_0 + I_i^{\max}} \right), \quad (9)$$

and

$$\begin{aligned} \bar{U}_i(\mathbf{p}_i) &\triangleq \begin{cases} K_i^1 \ln(1 + K_i^2 \ln(1 + (\bar{r}_i(\mathbf{p}_i) - r_i^{\min}))) & i \in \mathcal{S}_1 \cup \mathcal{S}_2, \\ K_i^3 \bar{r}_i(\mathbf{p}_i) & i \in \mathcal{S}_3. \end{cases} \end{aligned} \quad (10)$$

We then reformulate the non-convex MIP problem into the following minimization problem.

$$\text{minimize}_{\mathbf{x}, \mathbf{p}} - \sum_{i \in \mathcal{Q}} \bar{U}_i(\mathbf{p}_i) \quad (11a)$$

$$\text{subject to } \sum_{j \in \mathcal{Q} \setminus \{i\}} p_j^{t,c} G_{j,i} h_{j,i}^{t,c} \leq I_i^{\max}, \quad i \in \mathcal{Q}, t \in \mathcal{T}, c \in \mathcal{C}, \quad (11b)$$

$$\bar{r}_i(\mathbf{p}_i) \geq r_i^{\min}, \quad i \in \mathcal{Q}, \quad (11c)$$

$$\bar{r}_i(\mathbf{p}_i) \geq \xi \frac{L_{\text{slot}} - L_a}{L_{\text{sp}}} \sum_{t \in \mathcal{T}} \sum_{c \in \mathcal{C}} p_i^{t,c}, \quad i \in \mathcal{V}, \quad (11d)$$

constraints (8d)–(8f).

Problem (11) is an MIP problem with convex objective function. Compared with problem (8), the new constraint (11b) ensures that for each user, the received interference power is less than the estimated maximum interference. Constraints (11c) and (11d) are transformed into convex constraints with a smaller feasible region.

#### IV. OUTER APPROXIMATION BASED POWER AND CHANNEL ALLOCATION ALGORITHM

To solve problem (11), we use the OA method, which is a standard technique to solve convex MIP problems and provides their optimal solution [44], [45]. The convergence of OA method has been proven in [44]. The OA method solves

the convex MIP problem iteratively. Two problems, namely the *subproblem* and *master problem*, are involved in each iteration. The subproblem is a convex nonlinear programming (NLP) problem and the master problem is a mixed-integer linear programming (MILP) problem. The NLP subproblem is obtained from the original convex MIP problem by fixing the value of integer variables. The NLP subproblem provides an upper bound of the optimal value of the original convex MIP problem. The MILP master problem uses the solution of the NLP subproblem as an input, and provides a lower bound of the optimal value of the original convex MIP problem. We iteratively solve the subproblem and master problem until their solutions converge.

To use the OA method, we first transform problem (11) into a standard MIP format by simplifying the notation. We define

$$\begin{aligned} f(\mathbf{p}) &= - \sum_{i \in \mathcal{Q}} \bar{U}_i(\mathbf{p}_i), \\ \phi_i^{t,c}(\mathbf{p}) &= \sum_{j \in \mathcal{Q} \setminus \{i\}} p_j^{t,c} G_{j,i} h_{j,i}^{t,c} - I_i^{\max}, \quad i \in \mathcal{Q}, t \in \mathcal{T}, c \in \mathcal{C}, \\ \psi_i^1(\mathbf{p}_i) &= r_i^{\min} - \bar{r}_i(\mathbf{p}_i), \quad i \in \mathcal{Q}, \\ \psi_i^2(\mathbf{p}_i) &= \xi \frac{L_{\text{slot}} - L_a}{L_{\text{sp}}} \sum_{t \in \mathcal{T}} \sum_{c \in \mathcal{C}} p_i^{t,c} - \bar{r}_i(\mathbf{p}_i), \quad i \in \mathcal{V}. \end{aligned}$$

Then, problem (11) can be rewritten in the standard form as:

$$\text{minimize}_{\mathbf{x}, \mathbf{p}} f(\mathbf{p}) \quad (12a)$$

$$\text{subject to } \phi_i^{t,c}(\mathbf{p}) \leq 0, \quad i \in \mathcal{Q}, t \in \mathcal{T}, c \in \mathcal{C}, \quad (12b)$$

$$\psi_i^1(\mathbf{p}_i) \leq 0, \quad i \in \mathcal{Q}, \quad (12c)$$

$$\psi_i^2(\mathbf{p}_i) \leq 0, \quad i \in \mathcal{V}, \quad (12d)$$

constraints (8d)–(8f).

After transforming the original problem into the standard form, we can formulate the NLP subproblem and MILP master problem in each iteration. We denote  $k$  as the index of each iteration.

1) *NLP subproblem ( $k^{\text{th}}$  iteration)*: The NLP subproblem is obtained by fixing the value of binary variables  $\mathbf{x}$ . By doing so, the problem only consists of the continuous variables  $\mathbf{p}$ . In iteration  $k$ , given  $\mathbf{x}^{(k)}$  as a constant vector, the NLP subproblem is as follows:

$$\text{minimize}_{\mathbf{p}} f(\mathbf{p}) \quad (13a)$$

$$\text{subject to } 0 \leq p_i^{t,c} \leq x_i^{t,c(k)} p_i^{\max}, \quad i \in \mathcal{Q}, t \in \mathcal{T}, c \in \mathcal{C}, \quad (13b)$$

constraints (12b)–(12d).

Constraint (13b) is similar to (8d), where  $x_i^{t,c(k)}$  is given as a constant. In problem (13), the objective function and the constraints are all convex. Therefore, it is a convex problem which can be solved by using convex optimization solvers such as CVX [46]. We denote the optimal solution of problem (13) by  $\mathbf{p}^*$ . It is clear that the optimal value  $f(\mathbf{p}^*)$  obtained from problem (13) is an upper bound of the optimal value of problem (12). In order to find a lower bound of the original problem, we formulate the master problem.

2) *MILP master problem ( $k^{\text{th}}$  iteration)*: Both the objective function and the constraints in the master problem are based

on outer linearization [45]. If the value  $f(\mathbf{p}^*)$  obtained by solving the NLP subproblem is the tightest upper bound among all iterations, we use  $\mathbf{p}^*$  as the input  $\mathbf{p}^{(k)}$  to formulate the master problem. We introduce  $\varphi$  as an auxiliary variable to formulate the MILP problem. The solution of the MILP problem provides a lower bound of the original convex MIP problem [45, pp. 8]. The MILP master problem in iteration  $k$  is

$$\text{minimize } \varphi \quad (14a)$$

$$\text{subject to } f(\mathbf{p}^{(\hat{k})}) + \nabla f(\mathbf{p}^{(\hat{k})})(\mathbf{p} - \mathbf{p}^{(\hat{k})})^T \leq \varphi,$$

$$\hat{k} = 1, \dots, k, \quad (14b)$$

$$\phi_i^{t,c}(\mathbf{p}^{(\hat{k})}) + \nabla \phi_i^{t,c}(\mathbf{p}^{(\hat{k})})(\mathbf{p} - \mathbf{p}^{(\hat{k})})^T \leq 0,$$

$$i \in \mathcal{Q}, t \in \mathcal{T}, c \in \mathcal{C}, \hat{k} = 1, \dots, k, \quad (14c)$$

$$\psi_i^1(\mathbf{p}_i^{(\hat{k})}) + \nabla \psi_i^1(\mathbf{p}_i^{(\hat{k})})(\mathbf{p}_i - \mathbf{p}_i^{(\hat{k})})^T \leq 0,$$

$$i \in \mathcal{Q}, \hat{k} = 1, \dots, k, \quad (14d)$$

$$\psi_i^2(\mathbf{p}_i^{(\hat{k})}) + \nabla \psi_i^2(\mathbf{p}_i^{(\hat{k})})(\mathbf{p}_i - \mathbf{p}_i^{(\hat{k})})^T \leq 0,$$

$$i \in \mathcal{V}, \hat{k} = 1, \dots, k, \quad (14e)$$

constraints (8d)–(8f).

The gradient vectors in problem (14) are as follows:

$$\nabla f(\mathbf{p}^{(\hat{k})}) = - \frac{\eta B(L_{\text{slot}} - L_a)}{L_{\text{sp}} \ln 2} \left( \hat{\mathbf{C}}_1^{1,1}, \dots, \hat{\mathbf{C}}_i^{t,c}, \dots, \right. \\ \left. \hat{\mathbf{C}}_{|\mathcal{S}_1 \cup \mathcal{S}_2|}^{t,|\mathcal{C}|}, \bar{\mathbf{C}}_1^{1,1}, \dots, \bar{\mathbf{C}}_j^{t,c}, \dots, \bar{\mathbf{C}}_{|\mathcal{S}_3|}^{t,|\mathcal{C}|} \right), \quad (15)$$

where  $\hat{\mathbf{C}}_i^{t,c}, i \in \mathcal{S}_1 \cup \mathcal{S}_2, t \in \mathcal{T}, c \in \mathcal{C}$ , is

$$\hat{\mathbf{C}}_i^{t,c} = \left( 1 + K_i^2 \ln \left( 1 + \left( \eta B \frac{L_{\text{slot}} - L_a}{L_{\text{sp}}} \sum_{t \in \mathcal{T}} \sum_{c \in \mathcal{C}} \log_2 \left( 1 + \frac{G_0 h_{i,i}^{t,c} p_i^{t,c(\hat{k})}}{N_0 + I_i^{\max}} \right) - r_i^{\min} \right) \right) \right)^{-1} \left( 1 + \left( \eta B \frac{L_{\text{slot}} - L_a}{L_{\text{sp}}} \right. \right. \\ \left. \left. \times \sum_{t \in \mathcal{T}} \sum_{c \in \mathcal{C}} \log_2 \left( 1 + \frac{G_0 h_{i,i}^{t,c} p_i^{t,c(\hat{k})}}{N_0 + I_i^{\max}} \right) - r_i^{\min} \right) \right)^{-1} \\ \times \frac{K_i^1 K_i^2 G_0 h_{i,i}^{t,c}}{N_0 + I_i^{\max} + G_0 h_{i,i}^{t,c} p_i^{t,c(\hat{k})}}, \quad (16)$$

and  $\bar{\mathbf{C}}_j^{t,c}, j \in \mathcal{S}_3, t \in \mathcal{T}, c \in \mathcal{C}$ , is

$$\bar{\mathbf{C}}_j^{t,c} = \frac{K_j^3 G_0 h_{j,j}^{t,c}}{N_0 + I_j^{\max} + G_0 h_{j,j}^{t,c} p_j^{t,c(\hat{k})}}. \quad (17)$$

In addition,

$$\nabla \phi_i^{t,c}(\mathbf{p}^{(\hat{k})}) = \\ (G_{1,i}^{t,c} h_{1,i}^{t,c}, \dots, G_{i-1,i}^{t,c} h_{i-1,i}^{t,c}, 0, G_{i+1,i}^{t,c} h_{i+1,i}^{t,c}, \dots, G_{|\mathcal{Q}|,i}^{t,c} h_{|\mathcal{Q}|,i}^{t,c}), \quad (18)$$

and

$$\nabla \psi_i^1(\mathbf{p}_i^{(\hat{k})}) = \frac{-\eta B(L_{\text{slot}} - L_a) G_0}{L_{\text{sp}} \ln 2} \left( \check{\mathbf{C}}_i^1, \dots, \check{\mathbf{C}}_i^t, \dots, \check{\mathbf{C}}_i^{|\mathcal{T}|} \right), \quad (19)$$

where  $\check{\mathbf{C}}_i^t, i \in \mathcal{Q}, t \in \mathcal{T}$ , is defined as the  $t^{\text{th}}$  component in the gradient vector, and

$$\check{\mathbf{C}}_i^t = \left( \frac{h_{i,i}^{t,1}}{N_0 + I_i^{\max} + G_0 h_{i,i}^{t,1} p_i^{t,1(\hat{k})}}, \dots, \right. \\ \left. \frac{h_{i,i}^{t,|\mathcal{C}|}}{N_0 + I_i^{\max} + G_0 h_{i,i}^{t,|\mathcal{C}|} p_i^{t,|\mathcal{C}|(\hat{k})}} \right). \quad (20)$$

The gradient vector  $\nabla \psi_i^2(\mathbf{p}_i^{(\hat{k})})$  is

$$\nabla \psi_i^2(\mathbf{p}_i^{(\hat{k})}) = \left( \check{\mathbf{C}}_i^1, \dots, \check{\mathbf{C}}_i^t, \dots, \check{\mathbf{C}}_i^{|\mathcal{T}|} \right), \quad (21)$$

in which  $\check{\mathbf{C}}_i^t, i \in \mathcal{V}, t \in \mathcal{T}$ , is defined as the  $t^{\text{th}}$  component in the gradient vector, and

$$\check{\mathbf{C}}_i^t = \frac{L_{\text{slot}} - L_a}{L_{\text{sp}}} \left( \xi - \frac{\eta B G_0 h_{i,i}^{t,1}}{\ln 2 \left( N_0 + I_i^{\max} + G_0 h_{i,i}^{t,1} p_i^{t,1(\hat{k})} \right)}, \right. \\ \left. \dots, \xi - \frac{\eta B G_0 h_{i,i}^{t,|\mathcal{C}|}}{\ln 2 \left( N_0 + I_i^{\max} + G_0 h_{i,i}^{t,|\mathcal{C}|} p_i^{t,|\mathcal{C}|(\hat{k})} \right)} \right). \quad (22)$$

Note that the MILP master problem can be solved using standard optimization solvers such as MOSEK [47]. The MILP master problem has more constraints (i.e., the constraints added in the  $k^{\text{th}}$  iteration) compared to the one formulated in the previous iteration as shown in (14b)–(14e). Therefore, the lower bound of the optimal value of the convex MIP problem, which is obtained by solving the master problem, is tightened in each iteration. Similarly, by solving the subproblem and the master problem iteratively, the gap between the lower and upper bounds decreases. When the gap is smaller than a threshold, the solution of (12) is obtained.

The OA based scheduling and power allocation algorithm is shown in Algorithm 1. The proposed algorithm contains four steps. In the first step, we initialize the scheduling variables and power variables, the initial upper bound  $UB$ , and the initial lower bound  $LB$ , respectively (as shown in Line 1). In the second step, we solve NLP subproblem (13) to obtain solution  $\mathbf{p}$ . We update the current upper bound  $UB$  to be the minimum value of the previous  $UB$  and  $f(\mathbf{p})$  (as shown in Line 4). We then set the value of  $\mathbf{p}^{(k)}$  as  $\mathbf{p}$  (as shown in Line 5). In the third step, we solve MILP master problem (14). We update the lower bound by setting it as  $\varphi$  and set the value of  $\mathbf{x}^{(k+1)}$  as  $\mathbf{x}$  (as shown in Lines 7 and 8). Then, we set  $k := k + 1$ . In the fourth step, we evaluate the difference between the current upper bound  $UB$  and lower bound  $LB$ . If  $UB - LB \leq \varepsilon$ , the algorithm returns the optimal solution  $\mathbf{x}^*$  and  $\mathbf{p}^*$ . Otherwise, it returns to the second step (Line 3).

Compared with the generalized Benders decomposition method used in [37], although OA based algorithm has reduced the computational complexity of MIP problem (11), the complexity of Algorithm 1 is still very high due to the MILP problem in each iteration. MILP problems are generally NP-hard [48]. In particular, the worst-case complexity increases exponentially with the number of binary variables. The worst-case complexity of each iteration in the OA based algorithm

---

**Algorithm 1:** Integrated TDMA/FDMA/SDMA Resource Management based on OA Method

---

```

1 Initialize  $\mathbf{x}^{(1)}, \mathbf{p}^{(0)}, k := 1, UB := +\infty, LB := -\infty$ 
2 while  $UB - LB > \varepsilon$  do
3   Solve problem (13) to obtain solution  $\mathbf{p}$ 
4    $UB := \min(UB, f(\mathbf{p}))$ 
5    $\mathbf{p}^{(k)} := \mathbf{p}$ 
6   Solve problem (14) to obtain solution  $\mathbf{x}$  and optimal
   value  $\varphi$ 
7    $LB := \varphi$ 
8    $\mathbf{x}^{(k+1)} := \mathbf{x}$ 
9   Set  $k := k + 1$ 
10 end
11 output Scheduling decision  $\mathbf{x}^* = \mathbf{x}^{(k)}$  and optimal
   power  $\mathbf{p}^* = \mathbf{p}^{(k-1)}$ 

```

---

is  $O(2^{|\mathcal{Q}||\mathcal{T}||\mathcal{C}|})$ , which is the complexity of solving problem (14) in worst case. Thus, OA based algorithm is too complex for the real-time scheduling.

### V. GREEDY BASED HEURISTIC ALGORITHM

To overcome the computational complexity of the OA based algorithm, we propose a greedy based heuristic channel and power allocation algorithm in this section. The proposed heuristic greedy algorithm is shown in Algorithm 2. In this algorithm,  $\mathcal{Z}$  denotes the subset of links which require a minimum data rate. In the algorithm, we consider each time slot in a certain channel as a resource block (RB). We denote  $\Delta\bar{r}_i(\mathbf{x}_i, x_i^{t,c})$  as the estimated potential rate increment for link  $i$  if time slot  $t$  in channel  $c$  is allocated to it and maximum transmission power  $p^{\max}$  is used. We also define  $\Delta\bar{U}_i(\mathbf{x}_i, x_i^{t,c})$  as the estimated potential utility increment for link  $i$ .

The proposed algorithm separates the channel allocation and power allocation, which can reduce the computational complexity. There are three major steps in the algorithm. In the first step, we allocate the RBs to guarantee the minimum data rate requirements of the links, assuming the maximum power is used at the transmitting devices (Lines 2 to 14). Due to the directional communication, an RB can be shared by different links if the SINR requirements of all links are satisfied. Therefore, we find the link with the largest estimated rate increment and allocate the corresponding RB slot to that link (Lines 5 to 7). Specifically, we form set  $\mathcal{W}$  of indexes  $i, t$ , and  $c$ , subject to the conditions that RB  $t, c$  has not been allocated to link  $i$ , the interference requirement will be satisfied if RB  $t, c$  is allocated to this link, and no other channel is allocated in the same time slot (Line 3). Then, we sort the potential rate increment for different links and RBs in a non-increasing order (Line 5), and record  $i, t, c$  corresponding to the largest element of the sorted list (Line 6). In the second step, we allocate the RBs to all links by considering the utility increment (Lines 15 to 22). In each iteration, we allocate an RB to that link which results in the largest estimated network utility increment (Lines 17 to 21). The selection of the RBs

---

**Algorithm 2:** Integrated TDMA/FDMA/SDMA Resource Management based on Greedy Algorithm

---

```

1 Initialize  $\mathbf{p}_i := (p^{\max}, \dots, p^{\max}), i \in \mathcal{Q}, x_i^{t,c} := 0,$ 
    $i \in \mathcal{Q}, t \in \mathcal{T}, c \in \mathcal{C}$ 
2 while  $\mathcal{Z} \neq \emptyset$  do
3    $\mathcal{W} := \{(i, t, c) \in \{\mathcal{Z}, \mathcal{T}, \mathcal{C}\} \mid x_i^{t,c} = 0,$ 
    $\sum_{j \in \mathcal{Z} \setminus \{i\}} p^{\max} G_{j,i} h_{j,i}^{t,c} \leq I_i^{\max}, \sum_{c \in \mathcal{C}} x_i^{t,c} \leq 3\}$ 
4   if  $\mathcal{W} \neq \emptyset$  then
5     Sort  $\Delta\bar{r}_i(\mathbf{x}_i, x_i^{t,c}), (i, t, c) \in \mathcal{W}$  in a
     non-increasing order
6     Select the first element of the sorted list and
     record  $i, t, c$ 
7     Set  $x_i^{t,c} := 1$ 
8     if  $\bar{r}_i(\mathbf{p}_i) \geq r_i^{\min}$  then
9        $\mathcal{Z} := \mathcal{Z} \setminus \{i\}$ 
10    end
11  else
12    Return infeasible
13  end
14 end
15 do
16    $\tilde{\mathcal{W}} := \{(i, t, c) \in \{\mathcal{Q}, \mathcal{T}, \mathcal{C}\} \mid x_i^{t,c} = 0,$ 
    $\sum_{j \in \mathcal{Q} \setminus \{i\}} p^{\max} G_{j,i} h_{j,i}^{t,c} \leq I_i^{\max}, \sum_{c \in \mathcal{C}} x_i^{t,c} \leq 3,$ 
    $\Delta\bar{U}_i(\mathbf{x}_i, x_i^{t,c}) > 0\}$ 
17  if  $\tilde{\mathcal{W}} \neq \emptyset$  then
18    Sort  $\Delta\bar{U}_i(\mathbf{x}_i, x_i^{t,c}), (i, t, c) \in \tilde{\mathcal{W}}$  in a
    non-increasing order
19    Select the first element of the sorted list and
    record  $i, t, c$ 
20    Set  $x_i^{t,c} := 1$ 
21  end
22 while  $\tilde{\mathcal{W}} \neq \emptyset$ 
23 Given  $\mathcal{Q}, \mathcal{V}$ , and  $\bar{\mathbf{x}}^* = (x_i^{t,c})_{i \in \mathcal{Q}, t \in \mathcal{T}, c \in \mathcal{C}}$ , solve problem
   (23) to obtain  $\bar{\mathbf{p}}^*$  as the power allocation
24 output Channel and power allocation decision  $\bar{\mathbf{x}}^*$  and  $\bar{\mathbf{p}}^*$ 

```

---

and the links should also satisfy the constraint that a link cannot utilize multiple channels simultaneously. The second step terminates when  $\tilde{\mathcal{W}} = \emptyset$ . Now, we have allocated the channels and obtained channel allocation result  $\mathbf{x}$ . In the third step, we obtain the power of each transmitter by solving the following problem based on the obtained  $\mathbf{x}$ . The power allocation problem is as follows:

$$\underset{\mathbf{p}}{\text{maximize}} \sum_{i \in \mathcal{Q}} \bar{U}_i(\mathbf{p}_i) \quad (23a)$$

$$\text{subject to } \bar{r}_i(\mathbf{p}_i) \geq r_i^{\min}, \quad i \in \mathcal{Q}, \quad (23b)$$

$$\bar{r}_i(\mathbf{p}_i) \geq \xi \frac{L_{\text{slot}} - L_a}{L_{\text{sp}}} \sum_{t \in \mathcal{T}} \sum_{c \in \mathcal{C}} p_i^{t,c}, \quad i \in \mathcal{V}, \quad (23c)$$

$$0 \leq p_i^{t,c} \leq x_i^{t,c} p^{\max}, \quad i \in \mathcal{Q}, t \in \mathcal{T}, c \in \mathcal{C}. \quad (23d)$$

Problem (23) is a convex optimization problem and can be

TABLE II  
SIMULATION SETTINGS [8], [9], [35]

Parameter	Value
Frequency band	57.05 - 64.00 GHz
Bandwidth of each channel $B$	2.160 GHz
Noise power spectrum density $N_0/B$	-174 dBm/Hz
Maximum transmission power $p^{\max}$	10 dBm
Carrier frequency $f_{c1}, f_{c2}, f_{c3}$	58.32, 60.48, 62.64 GHz
Path loss reference distance $d_{bp}$	1 m
Attenuation of signals $A_{LOS}, A_{NLOS}$	7.1, 18 dB
Path loss exponent $n_{LOS}, n_{NLOS}$	2.0, 2.5
Shadowing standard deviation $\sigma_{LOS}, \sigma_{NLOS}$	1.5, 3.4
Length of scheduling period $L_{sp}$	65 ms
Length of beacon period $L_b$	0.3 ms
Length of control period $L_c$	5 ms
Pilots transmission duration $T_p$	655 ns
Sector level beam width $\Psi^{sr}, \Psi^{st}$	90°

solved by using convex optimization solvers. The optimal solution of this problem is denoted by  $\bar{p}^*$ . Finally, Algorithm 2 returns the channel and power allocation decision (Line 24).

In the following, we provide the complexity analysis of the greedy algorithm. In the first step of the algorithm from Lines 1 to 14, the number of iterations mainly depends on the size of set  $\mathcal{W}$ . Given  $|\mathcal{W}|$ , the complexity of sorting in Line 5 is  $O(|\mathcal{W}| \log(|\mathcal{W}|))$ , which is  $O(|\mathcal{Z}||\mathcal{T}||\mathcal{C}| \log(|\mathcal{Z}||\mathcal{T}||\mathcal{C}|))$  in worst case. Since the time required for executing the lines in the first step except Line 5 is constant, and the number of iterations executing the first step is  $O(|\mathcal{W}|)$ , the complexity of the first step is  $O(|\mathcal{W}|^2 \log(|\mathcal{W}|))$ . Similarly, the complexity of the second step (Lines 15 to 22) is  $O(|\widetilde{\mathcal{W}}|^2 \log(|\widetilde{\mathcal{W}}|))$ . Note that the convex problem (23) can be solved in polynomial time. Due to the fact that  $\mathcal{Z} \subseteq \mathcal{Q}$  and  $|\widetilde{\mathcal{W}}| \geq |\mathcal{W}|$ , the overall complexity of the algorithm is  $O(|\widetilde{\mathcal{W}}|^2 \log(|\widetilde{\mathcal{W}}|))$ , i.e.,  $O((|\mathcal{Q}||\mathcal{T}||\mathcal{C}|)^2 \log(|\mathcal{Q}||\mathcal{T}||\mathcal{C}|))$ . It can be seen that the complexity of the greedy algorithm is reduced compared to the OA based algorithm, which significantly improves its applicability for the real-time scheduling.

## VI. PERFORMANCE EVALUATION

In this section, we evaluate the performance of the proposed OA based and the greedy algorithms. We further compare both of the proposed algorithms with scalable heuristic STDMA scheduling (SHSS) algorithm [21] and vertex multi-coloring concurrent transmission (VMCCT) algorithm [32]. This is because [21] and [32] also focus on the spatial reuse in indoor mm-wave networks. The key differences between our algorithms and the algorithm proposed in [21] and [32] are that we further utilize mm-wave channelization and propose an OA based scheduling algorithm to maximize the aggregate utility for multimedia content delivery in mm-wave networks. We consider the transmitting devices are randomly located in the home with a uniform distribution. The receiving devices are randomly located with an average distance of 2 m around the transmitting devices. A random number of transmitting devices operate on battery. Their links form set  $\mathcal{V}$ . The service requested by each link is randomly selected from S1, S2, and S3. The parameters for the utility function are

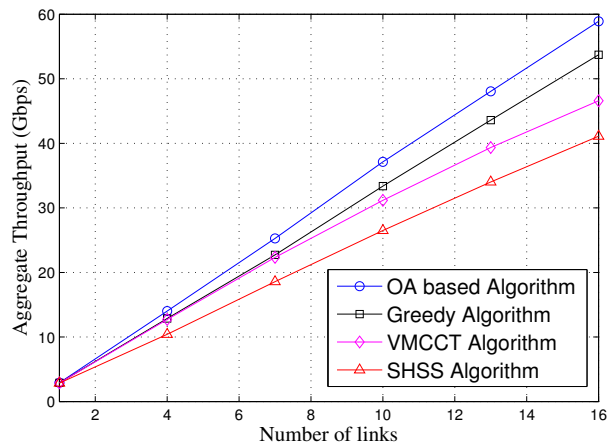


Fig. 5. Aggregate throughput versus number of links with the home area of 10 m × 10 m and  $\Theta_{3dB} = 15^\circ$ .

$K_i^1 = 1, K_i^2 = 0.7, r_i^{\min} = 0.95$  Gbps,  $i \in \mathcal{S}_1$ ;  $K_i^1 = 1.5, K_i^2 = 1, r_i^{\min} = 1.54$  Gbps,  $i \in \mathcal{S}_2$ ; and  $K_i^3 = 0.15, i \in \mathcal{S}_3$  [8]. The energy efficiency threshold  $\xi$  is  $10^5$  bit/joule [49]. The length of each time slot  $L_{slot}$  is  $(L_{sp} - L_b - L_c)/|\mathcal{T}|$ . Note that the number of time slots is equal to the number of links in the network<sup>2</sup>. Other simulation parameters are summarized in Table II [8], [9], [35]. We repeat the experiment using Monte Carlo simulations for each network setting, and calculate the average value of the performance metrics over different network settings.

We first compare the performance of our proposed algorithms with SHSS and VMCCT algorithms. Since SHSS and VMCCT algorithms aim to improve the throughput of the network using spatial reuse, we compare the algorithms in terms of throughput. In Fig. 5, we plot the aggregate throughput of the proposed OA based, greedy, SHSS, and VMCCT algorithms for different number of links in the network. Note that each link represents a pair of devices. Although the proposed algorithms aim to increase the network utility, they both achieve a higher aggregate throughput compared to the SHSS and VMCCT algorithms. This is because SHSS algorithm randomly selects the concurrent transmitting devices based on aggregate interference. However, we improve the spatial reuse by allocating the channels while considering the throughput and utility increment of each link. Moreover, VMCCT algorithm has a fixed exclusive region to forbid concurrent transmissions while we consider all possible concurrent transmissions to improve the spatial reuse.

In Fig. 6, we compare the aggregate throughput of our proposed algorithms with SHSS and VMCCT algorithms for different half power beam width  $\Theta_{3dB}$  to show the impact of alignment overhead. When the beam width is very narrow, the alignment overhead is dominant and reduces the overall

<sup>2</sup>According to the IEEE 802.15.3c and 802.11ad standards, the duration of a time slot can vary [35, pp. 26] [9, pp. 151, 178]. The duration of a time slot is determined based on transmission requests of active links. In our system, we assume all devices are active during the scheduling period and the total number of time slots is equal to the number of links. Since the duration of data transfer interval is the product of the duration of each time slot and the number of time slots, the duration of a time slot depends on the number of active links in the network.

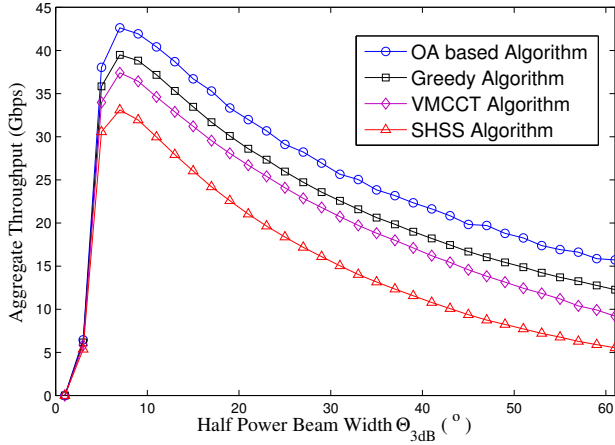


Fig. 6. Aggregate throughput versus half power beam width with the home area of  $10 \text{ m} \times 10 \text{ m}$ . The number of links  $|Q| = 10$ .

throughput. However, OA based and greedy algorithms always outperform SHSS and VMCCT algorithms.

We now evaluate the aggregate utility of OA based, greedy, SHSS, and VMCCT algorithms for different number of links in the network. As shown in Fig. 7, the aggregate utility of greedy algorithm is close to the OA based algorithm. Greedy algorithm achieves at least 90% of the aggregate utility of the OA based algorithm and outperforms VMCCT and SHSS algorithms by 22% and 39%, respectively, when the number of links is 16 and home area is  $100 \text{ m}^2$ . We also evaluate the aggregate utility of the proposed greedy algorithm for different home sizes. We compare the results for two different home sizes of  $144 \text{ m}^2$  and  $100 \text{ m}^2$ , respectively. As shown in this figure, a larger home size results in a slightly higher aggregate utility. This is due to the longer distance between the interfering devices in a larger home area. The highest utility is achieved with home area of  $144 \text{ m}^2$  with 16 links, which is close to the case of  $100 \text{ m}^2$ . Therefore, the proposed algorithms perform well in homes of different sizes.

In Fig. 8, we compare the performance of the proposed OA based, greedy, SHSS, and VMCCT algorithms when there is only one usage scenario in the network. Fig. 8 shows the aggregate network utility for three types of usage scenarios, where we fix the number of links to be 10. It is shown that the greedy algorithm achieves at least 90% of the aggregate utility compared to the OA based algorithm in different scenarios. In usage scenario S3, the aggregate utility of OA based and greedy algorithms is close to each other. This shows when the minimum data rate requirement is zero and the utility is a linear function of the effective throughput for scenario S3, the greedy algorithm is more likely to approach the optimal solution. Both OA based and greedy algorithms outperform the SHSS and VMCCT algorithms. Although the aggregate utility obtained by the OA based algorithm is slightly higher than greedy algorithm, we later present that the running time of the greedy algorithm is much less than the OA based algorithm.

In Fig. 9, we compare the average running time of OA based, greedy, SHSS, and VMCCT algorithms. Results show that the running time of the OA based algorithm is a couple of hundred seconds for each experiment. This degrades the applicability of the OA based algorithm when real-time scheduling

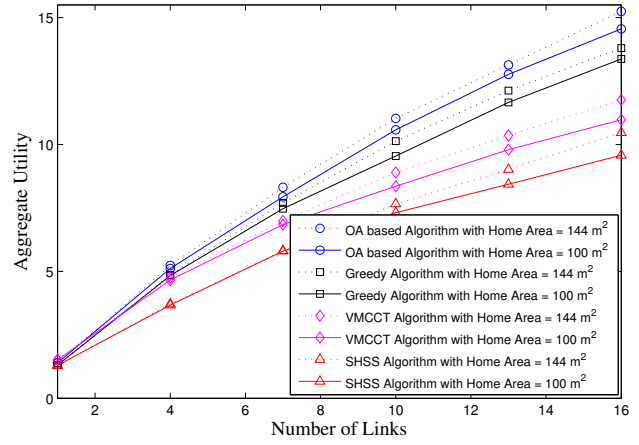


Fig. 7. Aggregate utility versus number of links with the home area of  $10 \text{ m} \times 10 \text{ m}$  and  $\Theta_{3\text{dB}} = 15^\circ$ .

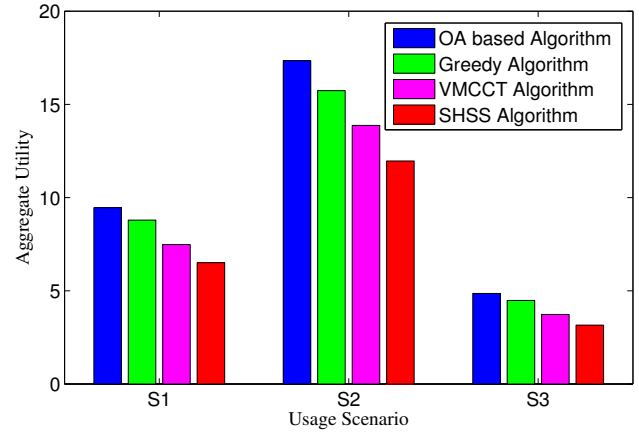


Fig. 8. Aggregate utility versus usage scenarios with the home area of  $10 \text{ m} \times 10 \text{ m}$ . The number of links  $|Q| = 10$ .

is needed. The running time of greedy algorithm is almost the same as SHSS and VMCCT algorithms, and is negligible compared to the running time of OA based algorithm. This demonstrates the efficiency of the proposed greedy algorithm.

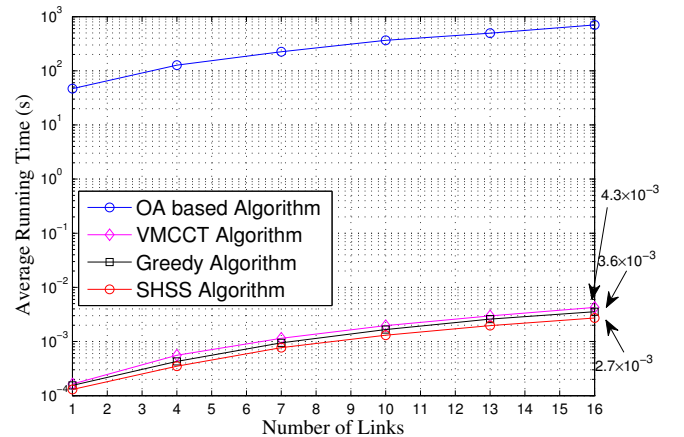


Fig. 9. Average running time versus number of links with the home area of  $10 \text{ m} \times 10 \text{ m}$ .

## VII. CONCLUSION

In this paper, we studied the resource management problem for multimedia content delivery in a mm-wave based smart home network. Specifically, we formulated a non-convex MIP optimization problem to maximize the aggregate network utility. We reformulated the problem into a convex MIP problem and designed an OA based algorithm to find the optimal solution of the reformulated problem. We further proposed a greedy algorithm with a lower computational complexity. Simulation results showed that both algorithms have substantial performance improvement compared to recently proposed algorithms in the literature. For future work, our work can be extended in several directions. First, we will consider contention-based transmission as a possible method for QoS-constrained applications with the limitation of guaranteed QoS to further improve the channel utilization when the device density is low. Second, our approach can be applied to other mm-wave based networks, such as future 5G systems. Third, a distributed algorithm can be considered when the number of devices is large.

## ACKNOWLEDGEMENT

The authors would like to thank Dr. Binglai Niu and Mr. Zehua Wang for their help and comments on simulations in the conference version of this paper.

## REFERENCES

- [1] N. Saito, "Ecological home network: An overview," *Proceedings of the IEEE*, vol. 101, no. 11, pp. 2428–2435, Nov. 2013.
- [2] T. S. Rappaport, R. W. Heath Jr, R. C. Daniels, and J. N. Murdock, *Millimeter Wave Wireless Communications*. Pearson Education, 2014.
- [3] T. S. Rappaport, S. Sun, R. Mayzus, H. Zhao, Y. Azar, K. Wang, G. Wong, J. Schulz, M. Samimi, and F. Gutierrez, "Millimeter wave mobile communications for 5G cellular: It will work!" *IEEE Access*, vol. 1, pp. 335–349, May 2013.
- [4] A. Ghosh, T. Thomas, M. Cudak, R. Ratasuk, P. Moorut, F. Vook, T. Rappaport, G. MacCartney, S. Sun, and S. Nie, "Millimeter-wave enhanced local area systems: A high-data-rate approach for future wireless networks," *IEEE J. on Selected Areas in Commun.*, vol. 32, no. 6, pp. 1152–1163, June 2014.
- [5] D. Wu, J. Wang, Y. Cai, and M. Guizani, "Millimeter-wave multimedia communications: Challenges, methodology, and applications," *IEEE Communications Magazine*, vol. 53, no. 1, pp. 232–238, Jan. 2015.
- [6] S. Scott-Hayward and E. Garcia-Palacios, "Multimedia resource allocation in mmWave 5G networks," *IEEE Communications Magazine*, vol. 53, no. 1, pp. 240–247, Jan. 2015.
- [7] T. Bai, A. Alkhatieb, and R. Heath, "Coverage and capacity of millimeter-wave cellular networks," *IEEE Communications Magazine*, vol. 52, no. 9, pp. 70–77, Sep. 2014.
- [8] IEEE Std 802.15.3c-2009, "IEEE standard for information technology-telecommunications and information exchange between systems-local and metropolitan area networks-specific requirements. Part 15.3: Wireless medium access control (MAC) and physical layer (PHY) specifications for high rate wireless personal area networks (WPANs) amendment 2: Millimeter-wave-based alternative physical layer extension," pp. 1–187, Oct. 2009.
- [9] IEEE 802.11 Working Group, "IEEE standard for information technology-telecommunications and information exchange between systems-local and metropolitan area networks-specific requirements-Part 11: Wireless LAN medium access control (MAC) and physical layer (PHY) specifications amendment 3: Enhancements for very high throughput in the 60 GHz band," *IEEE Std 802.11ad-2012*, pp. 1–628, Dec. 2012.
- [10] E. Charfi, L. Chaari, and L. Kamoun, "PHY/MAC enhancements and QoS mechanisms for very high throughput WLANs: A survey," *IEEE Communications Surveys Tutorials*, vol. 15, no. 4, pp. 1714–1735, Fourth Quarter 2013.
- [11] IEEE 802.11 Working Group, [http://www.ieee802.org/11/Reports/tgay\\_update.htm](http://www.ieee802.org/11/Reports/tgay_update.htm), 2015.
- [12] IEEE P802.11 Wireless LANs, "IEEE 802.11 TGay Use Cases," *IEEE 802.11-2015/0625r3*, Sep. 2015.
- [13] ISO/IEC/IEEE, "ISO/IEC/IEEE International Standard for Information technology-Telecommunications and information exchange between systems-Local and metropolitan area networks-Specific requirements-Part 11: Wireless LAN Medium Access Control (MAC) and Physical Layer (PHY) Specifications Amendment 3: Enhancements for Very High Throughput in the 60 GHz Band (adoption of IEEE Std 802.11ad-2012)," *ISO/IEC/IEEE 8802-11:2012/Amd.3:2014(E)*, pp. 1–634, Mar. 2014.
- [14] Y. Yiakoumis, K.-K. Yap, S. Katti, G. Parulkar, and N. McKeown, "Slicing home networks," in *Proc. of ACM SIGCOMM Workshop on Home Networks*, Toronto, Canada, Aug. 2011.
- [15] Y. He, J. Sun, R. Yuan, and W. Gong, "A reservation based backoff method for video streaming in 802.11 home networks," *IEEE J. on Selected Areas in Commun.*, vol. 28, no. 3, pp. 332–343, Mar. 2010.
- [16] T. Li, N. B. Mandayam, and A. Reznik, "A framework for distributed resource allocation and admission control in a cognitive digital home," *IEEE Trans. on Wireless Commun.*, vol. 12, no. 3, pp. 984–995, Mar. 2013.
- [17] S. Sundaresan, N. Feamster, and R. Teixeira, "Locating throughput bottlenecks in home networks," in *Proc. of ACM SIGCOMM*, Chicago, IL, Aug. 2014.
- [18] C.-Y. Li, C. Peng, G.-H. Tu, S. Lu, X. Wang, and R. Chandra, "Latency-aware rate adaptation in 802.11n home networks," in *Proc. of IEEE INFOCOM*, Hong Kong, China, Apr. 2015.
- [19] M. Park and P. Gopalakrishnan, "Analysis on spatial reuse and interference in 60-GHz wireless networks," *IEEE J. on Selected Areas in Commun.*, vol. 27, no. 8, pp. 1443–1452, Oct. 2009.
- [20] Q. Chen, X. Peng, J. Yang, and F. Chin, "Spatial reuse strategy in mmWave WPANs with directional antennas," in *Proc. of IEEE GLOBECOM*, Anaheim, CA, Dec. 2012.
- [21] C.-S. Sum and H. Harada, "Scalable heuristic STDMA scheduling scheme for practical multi-Gbps millimeter-wave WPAN and WLAN systems," *IEEE Trans. on Wireless Commun.*, vol. 11, no. 7, pp. 2658–2669, July 2012.
- [22] S. Singh, R. Mudumbai, and U. Madhoo, "Interference analysis for highly directional 60-GHz mesh networks: The case for rethinking medium access control," *IEEE/ACM Trans. on Networking*, vol. 19, no. 5, pp. 1513–1527, Oct. 2011.
- [23] J. Qiao, X. Shen, J. Mark, and Y. He, "MAC-layer concurrent beam-forming protocol for indoor millimeter-wave networks," *IEEE Trans. on Vehicular Technology*, vol. 64, no. 1, pp. 327–338, Jan. 2015.
- [24] G. Athanasiou, P. C. Weeraddana, C. Fischione, and L. Tassiulas, "Optimizing client association for load balancing and fairness in millimeter-wave wireless networks," *IEEE/ACM Trans. on Networking*, vol. 23, no. 3, pp. 836–850, June 2015.
- [25] H. Shokri-Ghadikolaei, C. Fischione, P. Popovski, and M. Zorzi, "Design aspects of short range millimeter wave networks: A MAC layer perspective," accepted for publication in *IEEE Network*, 2016.
- [26] I. K. Son, S. Mao, M. Gong, and Y. Li, "On frame-based scheduling for directional mmWave WPANs," in *Proc. of IEEE INFOCOM*, Orlando, FL, Mar. 2012.
- [27] J. Kim, Y. Tian, S. Mangold, and A. Molisch, "Joint scalable coding and routing for 60 GHz real-time live HD video streaming applications," *IEEE Trans. on Broadcasting*, vol. 59, no. 3, pp. 500–512, Sep. 2013.
- [28] K. Zheng, L. Zhao, J. Mei, M. Dohler, W. Xiang, and Y. Peng, "10 Gb/s HetSNETs with millimeter-wave communications: access and networking – challenges and protocols," *IEEE Comm. Magazine*, vol. 53, no. 1, pp. 222–231, Jan. 2015.
- [29] M. Di Renzo, "Stochastic geometry modeling and analysis of multi-tier millimeter wave cellular networks," *IEEE Trans. on Wireless Commun.*, vol. 14, no. 9, pp. 5038–5057, Sep. 2015.
- [30] Y. Niu, C. Gao, Y. Li, L. Su, D. Jin, and A. Vasilakos, "Exploiting device-to-device communications in joint scheduling of access and backhaul for mmwave small cells," *IEEE J. on Selected Areas in Commun.*, vol. 33, no. 10, pp. 2052–2069, Oct. 2015.
- [31] J. Qiao, X. S. Shen, J. W. Mark, Q. Shen, Y. He, and L. Lei, "Enabling device-to-device communications in millimeter-wave 5G cellular networks," *IEEE Communications Magazine*, vol. 53, no. 1, pp. 209–215, Jan. 2015.
- [32] W. U. Rehman, J. Han, C. Yang, M. Ahmed, and X. Tao, "On scheduling algorithm for device-to-device communication in 60 GHz networks," in *Proc. of IEEE WCNC*, Istanbul, Turkey, Apr. 2014.
- [33] J. Guillory, E. Tanguy, A. Pizzinat, B. Charbonnier, S. Meyer, C. Algani, and H. Li, "A 60 GHz wireless home area network with radio over fiber

repeaters,” *Journal of Lightwave Technology*, vol. 29, no. 16, pp. 2482–2488, Aug. 2011.

- [34] N. Moraitis and P. Constantinou, “Indoor channel measurements and characterization at 60 GHz for wireless local area network applications,” *IEEE Trans. on Antennas and Propagation*, vol. 52, no. 12, pp. 3180–3189, Dec. 2004.
- [35] IEEE P802.15 Working Group for Wireless Personal Area Networks, “TG3c channel modeling sub-committee final report,” *IEEE 802.15-0584-003c*, Mar. 2007.
- [36] IEEE P802.11 Working Group AD, “Channel models for 60 GHz WLAN systems,” *IEEE 802.11-09/0334r8*, May 2010.
- [37] B. Ma, B. Niu, Z. Wang, and V. W. S. Wong, “Joint power and channel allocation for multimedia content delivery using millimeter wave in smart home networks,” in *Proc. IEEE GLOBECOM*, Austin, TX, Dec. 2014.
- [38] L. Wang, J. Chen, X. Wei, J. Cui, and B. Zheng, “First-order-reflection MIMO channel model for 60 GHz NLOS indoor WLAN systems,” in *Proc. of IEEE Int’l Conf. on Communication Systems (ICCS)*, Macau, China, Nov. 2014.
- [39] A. Alkhateeb, O. El Ayach, G. Leus, and R. W. Heath, “Channel estimation and hybrid precoding for millimeter wave cellular systems,” *IEEE J. of Selected Topics in Signal Processing*, vol. 8, no. 5, pp. 831–846, July 2014.
- [40] I. Toyoda, T. Seki, K. Iigusa, H. Sawada, Y. Fujita, A. Miura, and N. Orihashi, “Reference antenna model with side lobe for TG3c evaluation,” *IEEE 802.15-06-0474-00-003c*, Mar. 2007.
- [41] H. Shokri-Ghadikolaei, L. Gkatzikis, and C. Fischione, “Beam-searching and transmission scheduling in millimeter wave communications,” in *Proc. of IEEE ICC*, London, UK, June 2015.
- [42] R. R.-F. Liao and A. T. Campbell, “A utility-based approach for quantitative adaptation in wireless packet networks,” *Wireless Networks*, vol. 7, no. 5, pp. 541–557, Sep. 2001.
- [43] H. Shokri-Ghadikolaei and C. Fischione, “The transitional behavior of interference in millimeter wave networks and its impact on medium access control,” *IEEE Trans. on Commun.*, vol. 64, no. 2, pp. 723–740, Feb. 2016.
- [44] M. A. Duran and I. E. Grossmann, “An outer-approximation algorithm for a class of mixed-integer nonlinear programs,” *Mathematical Programming*, vol. 36, no. 3, pp. 307–339, Dec. 1986.
- [45] R. Fletcher and S. Leyffer, “Solving mixed integer nonlinear programs by outer approximation,” *Mathematical Programming*, vol. 66, no. 3, pp. 327–349, Aug. 1994.
- [46] M. Grant, S. Boyd, and Y. Ye, “CVX: Matlab software for disciplined convex programming, version 2.1,” Mar. 2015.
- [47] “The MOSEK optimization software,” <https://www.mosek.com>, 2015.
- [48] M. R. Garey and D. S. Johnson, *Computers and Intractability: A Guide to the Theory of NP-Completeness*. San Francisco, LA: Freeman, 1979.
- [49] G. Miao, N. Himayat, and G. Li, “Energy-efficient link adaptation in frequency-selective channels,” *IEEE Trans. on Commun.*, vol. 58, no. 2, pp. 545–554, Feb. 2010.



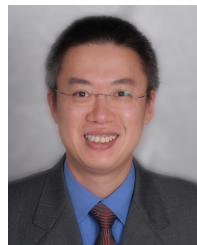
**Bojiang Ma** (S’13) received the B.Eng. degree from Southeast University, Nanjing, JiangSu, China, in 2009, and M.A.Sc. degree from University of Victoria, Victoria, BC, Canada in 2011. He is currently working towards the Ph.D. degree at the University of British Columbia, Vancouver, BC, Canada. His research interests include interference management and resource allocation for heterogeneous wireless networks using optimization theory and game theory, with current focus on small cell networks, home wireless networks, and mm-wave communication

systems.



**Hamed Shah-Mansouri** (S’06-M’14) received the B.Sc., M.Sc., and Ph.D. degrees from Sharif University of Technology, Tehran, Iran, in 2005, 2007, and 2012, respectively all in electrical engineering. He ranked first among the graduate students. From 2012 to 2013, he was with Parman Co., Tehran, Iran. Currently, Dr. Shah-Mansouri is a post-doctoral research and teaching fellow at the University of British Columbia, Vancouver, Canada. His research interests are in the area of stochastic analysis, optimization and game theory and their applications

in economics of cellular networks and mobile cloud computing systems. He has served as the publication co-chair for the IEEE Canadian Conference on Electrical and Computer Engineering 2016 and as the technical program committee (TPC) member for several conferences including the IEEE Global Communications Conference (GLOBECOM) 2015 and the IEEE Vehicular Technology Conference (VTC2016-Fall).



**Vincent W.S. Wong** (S’94, M’00, SM’07, F’16) received the B.Sc. degree from the University of Manitoba, Winnipeg, MB, Canada, in 1994, the M.A.Sc. degree from the University of Waterloo, Waterloo, ON, Canada, in 1996, and the Ph.D. degree from the University of British Columbia (UBC), Vancouver, BC, Canada, in 2000. From 2000 to 2001, he worked as a systems engineer at PMC-Sierra Inc. He joined the Department of Electrical and Computer Engineering at UBC in 2002 and is currently a Professor. His research areas include

protocol design, optimization, and resource management of communication networks, with applications to wireless networks, smart grid, and the Internet. Dr. Wong is an Editor of the *IEEE Transactions on Communications*. He is a Guest Editor of *IEEE Journal on Selected Areas in Communications*, special issue on “Emerging Technologies” in 2016. He has served on the editorial boards of *IEEE Transactions on Vehicular Technology* and *Journal of Communications and Networks*. He has served as a Technical Program Co-chair of *IEEE SmartGridComm’14*, as well as a Symposium Co-chair of *IEEE SmartGridComm’13* and *IEEE Globecom’13*. He is the Chair of the IEEE Communications Society Emerging Technical Sub-Committee on Smart Grid Communications and the IEEE Vancouver Joint Communications Chapter. He received the 2014 UBC Killam Faculty Research Fellowship.